Associations of Lithium Alkyl Dicarbonates through O···Li···O Interactions

Yixuan Wang* and Perla B. Balbuena*

Department of Chemical Engineering, Swearingen Engineering Center, University of South Carolina, Columbia, South Carolina 29208

Received: June 18, 2002; In Final Form: August 22, 2002

Associations of several lithium alkyl (vinylene, divinylene, ethylene, and propylene) dicarbonates, resulting from the reductive decomposition of organic carbonates and playing a crucial role on the formation of a solid electrolyte interphase (SEI) in rechargeable Li-ion batteries, have been extensively investigated with density functional theory methods. Lithium alkyl dicarbonates can associate through intermolecular O···Li···O interactions. For their dimers, the cagelike isomer is the most stable structure. Closed pseudoplanar structures turn out to be the global minima for trimers as well as for tetramers. O···Li···O interactions have been characterized with atoms-in-molecules (AIM) and natural bond order (NBO) analysis, and it is found that Li···O behave as ionic interactions. It has also been found that the partial charges of Li ions are decreased in the range of 0.004e to 0.035e when O···Li···O interactions occur or when a Li atom is being shared by more adjacent oxygen atoms, whereas the overall NBO bond orders of Li are considerably increased. Moreover, the BSSE-corrected binding energies of the associates linearly correlate with the total variations of bond orders of all the involved Li ions. The effects of associations on the IR spectra have also been investigated. Both the energetics and IR spectra of lithium alkyl dicarbonates association indicate that lithium alkyl dicarbonates exist on the anode surface, forming 2-dimensional *n*-mers and even 3-dimensional ones rather than monomers.

1. Introduction

With the impressive growth in sales of Li-ion batteries worldwide, an enhanced understanding of the science underlying Li-ion battery technology, e.g., Li chemistry, is becoming more and more crucial to improve performances and optimize components of Li-ion batteries.[1] The cycle life, stability, and other relevant performances of a lithium-ion rechargeable battery, consisting of a graphitic carbon anode, a nonaqueous organic electrolyte and a transition metal oxide (such as $LiCoO_2$, $LiMn_2O_4$, and $LiNiO_2$) cathode, depend greatly on the formation of an efficient solid electrolyte interphase (SEI) layer between the graphite anode surface and the electrolyte, which is mainly attributed to the reductive decomposition of the organic carbonate electrolyte during the first several cycles. A lot of effort by experimentalists as well as by theoreticians has been devoted to exploring the SEI formation mechanism and to characterize its components. Because of its intrinsic complexity, the explanations for the SEI formation mechanism and its chemical composition provided by various research groups are still controversial. However, advanced techniques such as in situ Fourier transform infrared spectroscopy (FTIR), and X-ray photoelectron spectroscopy (XPS),[2] in the case of ethylene carbonate (EC)-based electrolyte, e.g., mixtures of EC with linear carbonates such as dimethyl carbonate (DMC) and diethyl carbonate (DEC), have identified lithium ethylene dicarbonate, $LiO_2COCH_2CH_2OCO_2Li$ or $(CH_2OCO_2Li)_2$, as major SEI components. Although not as well recognized as $(CH_2OCO_2Li)_2$, another lithium alkyl dicarbonate with a bigger alkyl group, $-(CH_2)_4-$, $(CH_2CH_2OCO_2Li)_2$, sometimes is suggested in EC-based solutions (EC−DMC−$LiAsF_6$, highly oriented pyrolytic graphite; EC−$LiClO_4$, natural graphite).[3,4] Besides the two compounds, a Li carbide containing a Li−C bond, $Li-CH_2-CH_2OCO_2Li$, was also found on the electrode surface by XPS.[2,3] At low EC concentration an inorganic compound, Li_2CO_3, could dominate on the electrode surface.[5] Theoretical studies on the electroreductive decomposition of EC basically support these identifications,[6] although the theoretically predicted product, $LiO(CH_2)_2CO_2(CH_2)_2OCO_2Li$, has not yet been experimentally identified as an SEI component.

Except for the presence of a different alkyl group ($-CH_2-CH_2-$ vs $-CH(CH_3)CH_2-$), the electroreduction products of propylene carbonate (PC) are quite similar to those of EC.[7] Lithium propylene dicarbonate, $CH_3CH(OCO_2Li)CH_2(OCO_2Li)$, could become deposited on the Li surface, building up an appropriate SEI.[8,9] Similarly, the possibility of a longer alkyl dicarbonate, 2,3-dimethyllithium butylene dicarbonate, $(CH_3CHCH_2OCO_2Li)_2$, as a SEI layer species on lithium surfaces was also suggested by Aurbach et al. on the basis of the fact that the percentage of the alkyl carbon XPS peak around 285−286 eV is much higher than that expected from lithium propylene dicarbonate.[8]

As carbon materials are used as the anode of Li-ion batteries, the addition of small amounts of highly reactive compounds, such as vinylene carbonate (VC),[10,11] to EC/PC-based electrolyte solutions currently is an efficient way to improve the SEI film in EC solutions or to build up an appropriate SEI film in PC solutions. Although the functioning mechanism of the compounds that adequately perform the additive role is not totally unambiguous, it seems that having a higher reduction potential than EC and PC, i.e., preferential reduction on the electrode surface, plays an important role, generating a more stable precursor, which will undergo a homolytic ring-opening and lead to the formation of the SEI layer components, although

* Corresponding authors. E-mails: wangyi@engr.sc.edu, balbuena@engr.sc.edu.

10.1021/jp026329j CCC: $22.00
Published on Web 09/24/2002

the energy barrier for the homolytic ring-opening reactions of VC is nearly 1 time higher than those for EC and PC.[7,12] This implies that the thermodynamics aspects dominate the VC role as an electrolyte additive. On the other hand, because of the presence of the double bond, reduction products of VC such as lithium alkyl dicarbonates, $LiOCO_2(CH{=}CH)_nOCO_2Li$ ($n = 1$, 2), perhaps aggregate to a larger extent than those from EC or PC and/or polymerize on the electrode surface to generate polymeric or oligomeric species, which are more cohesive and flexible, and thus form a more efficient SEI layer.[13] Moreover, the presence of VC might also suppress cointercalation of EC/PC molecules,[7,14] which has been considered as a main cause of PC's destruction of the graphite electrode in Li-ion batteries.[15−17]

In the present study, density functional theory is applied to the main reduction products of VC, EC, and PC, focusing upon (i) their associations, i.e., geometrical structures and energetics of these aggregates, (ii) the effect of their associations on the infrared spectroscopy, one of the main techniques that has been used to identify SEI components, and (iii) the nature of O···Li···O_x ($x > 1$) interactions, and the relationships between the binding energies and the variations of atomic partial charges, as well as the overall bond orders. These results provide useful insights into the possible appearance of these lithium dicarbonates when they are part of the SEI film and help in the assignment of the experimental FTIR. In the course of comparing the present results with experimental FTIR, eventually we will try to discuss several important issues relevant to the SEI layer formation and chemical composition.

2. Computational Details

All the calculations have been performed using the G98 version A9 program, where the Gaussian NBO version 3.1 has been implemented.[18] For the aggregates of lithium alkyl dicarbonate, a large number of conformers exist for rotation around the O−C (carbonyl) bonds; therefore the conformational space of all ground states was first explored at the lower HF/3-21G level and then reoptimized at the higher B3PW91/4-31G level.[19−22] For the conformers with similar energies, the basis set superposition error (BSSE) corrections were estimated using the counterpoise method of Boys and Bernardi:[23]

$$\mathrm{BSSE(dimer)} = E(\mathrm{A})_{\mathrm{A}} - E(\mathrm{A})_{\mathrm{AB}} + E(\mathrm{B})_{\mathrm{B}} - E(\mathrm{B})_{\mathrm{AB}}$$

$$\mathrm{BSSE(trimer)} = E(\mathrm{A})_{\mathrm{A}} - E(\mathrm{A})_{\mathrm{ABC}} + E(\mathrm{B})_{\mathrm{B}} - E(\mathrm{B})_{\mathrm{ABC}} + E(\mathrm{C})_{\mathrm{C}} - E(\mathrm{C})_{\mathrm{ABC}}$$

$$\mathrm{BSSE(tetramer)} = E(\mathrm{A})_{\mathrm{A}} - E(\mathrm{A})_{\mathrm{ABCD}} + E(\mathrm{B})_{\mathrm{B}} - E(\mathrm{B})_{\mathrm{ABCD}} + E(\mathrm{C})_{\mathrm{C}} - E(\mathrm{C})_{\mathrm{ABCD}} + E(\mathrm{D})_{\mathrm{D}} - E(\mathrm{D})_{\mathrm{ABCD}}$$

where $E(\mathrm{A})_{\mathrm{AB}}$ [or $E(\mathrm{A})_{\mathrm{ABC}}$ and $E(\mathrm{A})_{\mathrm{ABCD}}$] refers to the energy of the monomer calculated by using its geometry within the dimer (or the trimer and the tetramer) and the complete set of basis functions describing the dimer (or the trimer and the tetramer), and $E(\mathrm{A})_{\mathrm{A}}$ uses the same geometry as $E(\mathrm{A})_{\mathrm{AB}}$ but only the basis set of itself. Finally, the most favorable conformer after BSSE was reoptimized by the B3PW91/6-31G(d), and frequency analyses were done with the same basis sets to confirm the equilibrium structures and make zero point energy (ZPE) corrections for most of species. If not noted otherwise, relative energies refer to those without ZPE correction, and enthalpies and Gibbs free energies are calculated at 298.2 K. The charge distributions have been characterized with Mulliken as well as with natural population analyses (NPA),[24] and by fitting the molecular electrostatic potential to atomic point charges using the CHELPG method.[25] The bond orders are calculated by a full natural bond orbital analysis (NBO).[24] To gain insight into the bonding characteristics between Li^+ and oxygen, the atoms-in-molecules (AIM) theory of Bader[26] is applied to most of the species. AIM is based on a topological analysis of the electron density function $\rho(r)$ and of its Laplacian $\nabla^2\rho(r)$ at the bond critical point (bcp). It is well established that the interactions between closed-shell systems (ionic bond, hydrogen bond, van der Waals interactions, etc.) demonstrate a low $\rho(r)$ value and $\nabla^2\rho(r) > 0$, whereas high $\rho(r)$ and $\nabla^2\rho(r) < 0$ correspond to covalent bonds.

3. Results and Discussion

3.1. Geometries and Energetics. *Lithium Vinylene Dicarbonate (LVD) $(CHOCO_2Li)_2$.* The optimized structures are illustrated in Figure 1 together with selected structural data, bond orders, and $\nabla^2\rho(r)$. The partial atomic charges depend much on the methodologies. The partial charge of Li in **1a**, for example, ranges from +0.57e (Mulliken) over +0.82e (CHELPG) to +0.93e (NPA), and those of the two carbonate O atoms (O1, O2) linked with Li are −0.64, −0.63e (Mulliken), −0.78, −0.79e (CHELPG), and −0.83, −0.86e (NPA), respectively. The NPA results will be used throughout the following discussions. AIM calculations show that there is a bond critical point (bcp) between Li and O1 ($\rho(r) = 0.036$e, $\nabla\ ^2\rho(r) = 0.287$au), as well as O2 ($\rho(r) = 0.035$e, $\nabla^2\rho(r) = 0.277$au), respectively, and the corresponding NBO bond orders (atom−atom overlap-weighted natural analysis orbital bond order) are 0.118 and 0.109. Consequently, a ring critical point ($\rho(r) = 0.036$e) exists for the four-membered ring consisting of Li, O1, O2, and C (carbonyl carbon). AIM results together with NPA partial charges reveal that an ionic bond does exist between Li and O1 and O2, respectively.

Although intermolecular C−H···O interactions have been well established for molecules containing C−H and carbonyl groups,[27] the corresponding aggregates were not located for lithium vinylene dicarbonate. As illustrated in Figure 1 (**1b**, **1c** and **1d**), the head-to-end, side-by-side, and cage types of dimers are found through intermolecular O···Li···O interactions, where Li ions are shared by two molecules. In the chain dimer **1b**, Li separates from one of the linking O atoms in lithium vinylene dicarbonate (the distance is ∼2.23 Å; the bond order is ∼0.058) and combines with another O of the second LVD, resulting in an eight-membered ring with two identical O···Li···O interactions (∠O···Li···O = 162.0°), where one O···Li is dramatically contracted by 0.06 Å (1.804 Å) and the other is slightly stretched by 0.01 Å (1.889 Å) relative to the LVD monomer. The geometric parameters of the carbonate group change slightly; for example, CO1 and CO3 are only contracted by 0.013 Å (1.254 vs 1.267 Å) and by 0.005 Å (1.351 vs 1.356 Å), and CO2 is stretched by 0.004 Å (1.266 vs 1.262 Å). The side-by-side dimer **1c** displays a cyclic structure, where two new Li···O bonds appear (distance ∼1.961 Å, bond order, 0.098). Although other Li···O bonds are also considerably stretched, especially for the two Li donor moieties (1.965, 1.959 Å vs 1.888, 1.895 Å of Li acceptor moieties), each LVD well retains its original structure. The LVD molecule dramatically deforms in dimer **1d** to adopt the cage structure. Moreover, in contrast to **1b** and **1c**, four quasi-degenerate O···Li···O (∠O···Li···O = 148.6−149.9°) interactions emerge in **1d**, where the contracted Li···O bond lengths are 1.824−1.825 Å, and the stretched ones are in the range of 1.900 and 1.903 Å. As a result of four O···Li···O interactions, **1d** has significantly lower energy than **1b** and **1c**, and their binding energies with ZPE and BSSE corrections are 67.1, 42.8, and 37.0 kcal/mol, respectively.

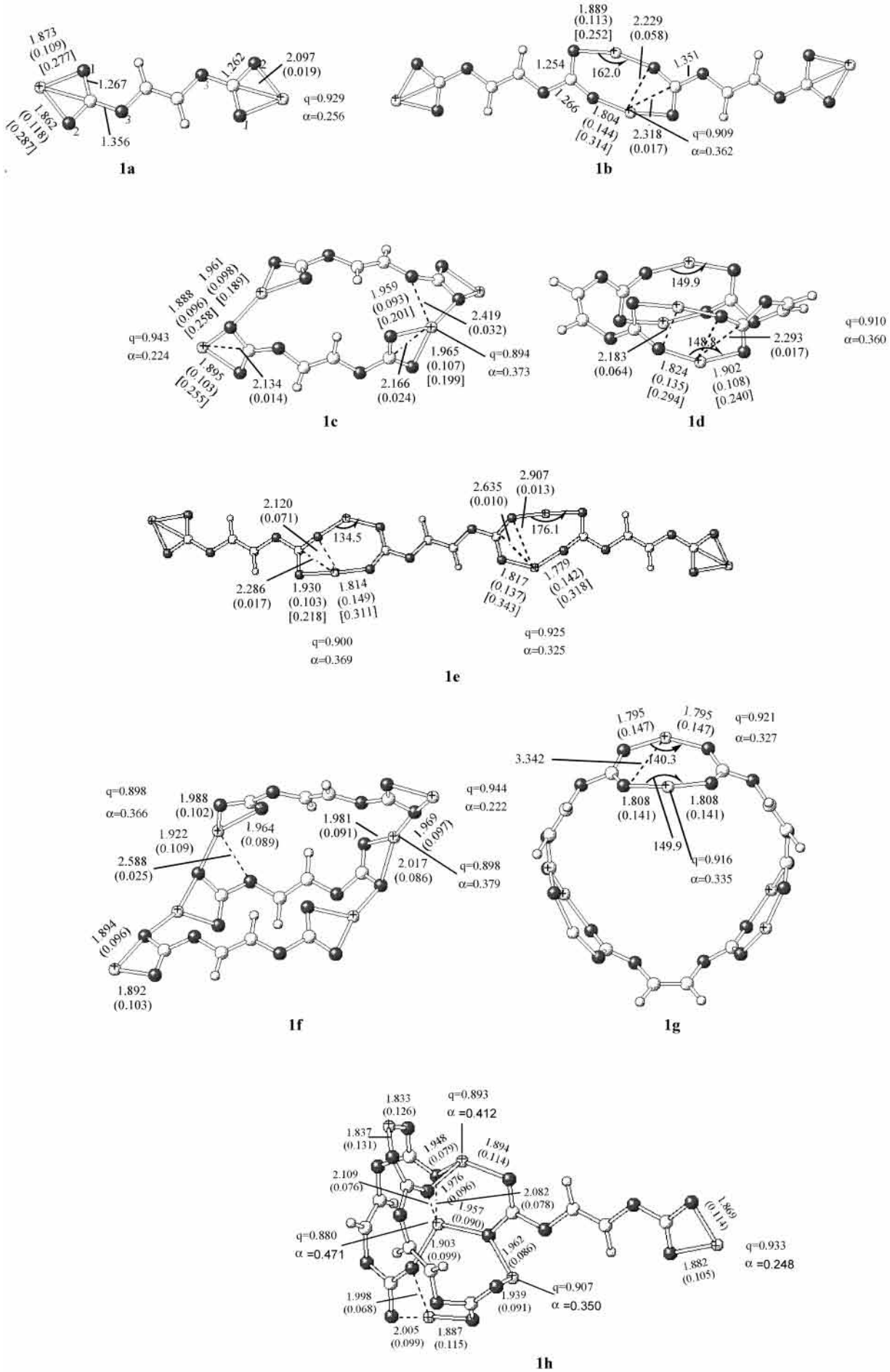
1.873 (0.109) [0.277]
1.267
1.262
2.097 (0.019)
q=0.929
α=0.256
1.862 (0.118) [0.287]
1.356
1a
1.889 (0.113) [0.252]
2.229 (0.058)
1.254
162.0
1.351
1.266
1.804 (0.144) [0.314]
2.318 (0.017)
q=0.909
α=0.362
1b
1.961 (0.098) [0.189]
1.888 (0.096) [0.258]
1.959 (0.093) [0.201]
2.419 (0.032)
q=0.943
α=0.224
1.965 (0.107) [0.199]
q=0.894
α=0.373
1.895 (0.103) [0.255]
2.134 (0.014)
2.166 (0.024)
1c
149.9
148.8
2.293 (0.017)
q=0.910
α=0.360
2.183 (0.064)
1.824 (0.135) [0.294]
1.902 (0.108) [0.240]
1d
2.907 (0.013)
2.635 (0.010)
2.120 (0.071)
134.5
176.1
2.286 (0.017)
1.930 (0.103) [0.218]
1.814 (0.149) [0.311]
1.817 (0.137) [0.343]
1.779 (0.142) [0.318]
q=0.900
α=0.369
q=0.925
α=0.325
1e
1.795 (0.147)
1.795 (0.147)
q=0.921
α=0.327
3.342
140.3
1.808 (0.141)
1.808 (0.141)
149.9
q=0.916
α=0.335
1g
q=0.898
α=0.366
1.988 (0.102)
1.964 (0.089)
1.922 (0.109)
1.981 (0.091)
1.969 (0.097)
q=0.944
α=0.222
2.588 (0.025)
2.017 (0.086)
q=0.898
α=0.379
1.894 (0.096)
1.892 (0.103)
1f
1.833 (0.126)
q=0.893
α =0.412
1.837 (0.131)
1.948 (0.079)
1.894 (0.114)
2.109 (0.076)
1.976 (0.096)
2.082 (0.078)
1.957 (0.090)
1.869 (0.114)
q=0.880
α =0.471
1.903 (0.099)
1.962 (0.086)
q=0.933
α =0.248
1.882 (0.105)
1.998 (0.068)
q=0.907
α =0.350
1.939 (0.091)
2.005 (0.099)
1.887 (0.115)
1h

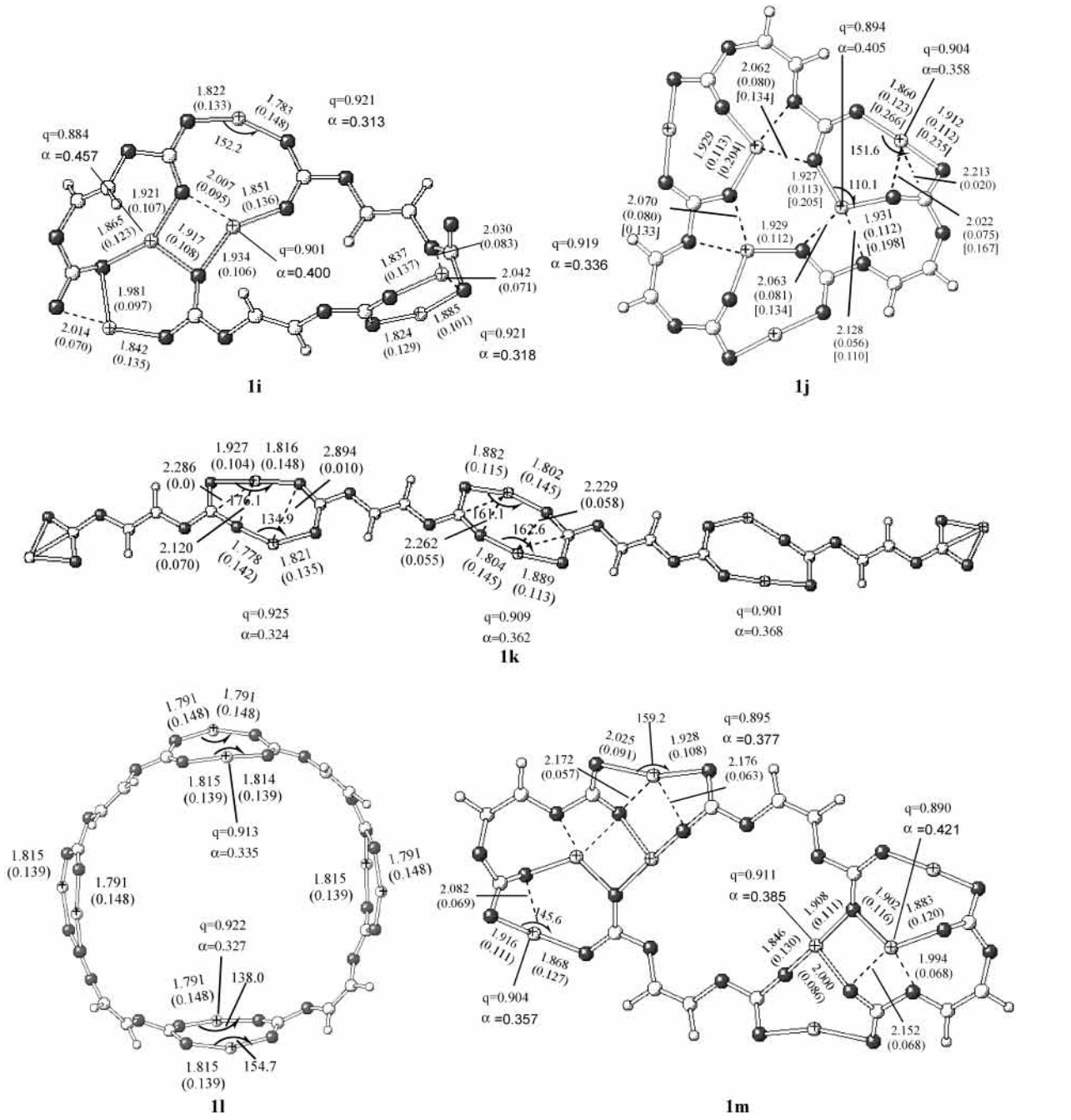

Figure 1. Structures with selected parameters by B3PW91/6-31G*: (**1a**) lithium vinylene dicarbonate; (**1b**−**1d**) dimer; (**1e**−**1j**) trimer; (**1k**−**1m**) tetramer. Solid balls stand for oxygen atoms, big empty ones for carbon atoms, small empty ones for hydrogen atoms, and the balls marked with a plus for lithium atoms. The numbers in parentheses refer to overall bond order with NBO-B3PW91/6-31G, and those in brackets to $\nabla^2\rho(r)$ at the bond critical points with AIM-B3PW91/6-31G*. *q* and α are the partial charges and total overall bond orders of Li ions with NBO-B3PW91/6-31G, respectively.

In general, the trimers of lithium vinylene dicarbonate could be classified into open and closed structures. The open structures **1e**, **1f,** and **1h**, where one or two end Li ions are not shared by two molecules, could be considered as the attachment of one more LVD to **1b** in the way of head-to-end, to **1c** in side-by-side, to **1c** in head-to-end or to **1b** in side-by-side, respectively. In **1e**, O···Li···O interactions are quite different from those in **1b**. Two O···Li···O are very bent with an angle of 134.5°, and their two O···Li distances are considerably contracted (1.778 and 1.817 Å), whereas another two O···Li···O tend to achieve linear orientation (176°) with one contracted O···Li (1.814 Å) and the other stretched O···Li (1.930 Å) relative to the monomer. Except for the additional LVD, **1f** looks rather like dimer **1c**, and intermolecular O···Li distances are in the range 1.92−1.97 Å. Three main closed structures were found, including cagelike **1g**, pseudoplanar **1j**, and that between **1i**. The process of formation of **1i** could be thought of as initially rolling of **1e**, resulting in a cagelike structure (not shown) that is indeed a local minimum at HF/4-31G and B3PW91/4-31G levels, and then isomerizing to the current structure by further intramolecular O···Li···O interactions. **1g** has C_{3v} symmetry with only two kinds of O···Li···O interactions, in which ∠O···Li···O and O···Li are 140.3°, 1.795 Å and 149.9°, 1.808 Å, respectively. In the case of **1j**, the three outer O···Li···O interactions tend to be rather flat (∠O···Li···O ∼ 152°) with two long O···Li bonds (1.91 and 1.86 Å), whereas the inner interactions are very bent (∠O···Li···O ∼ 110°) and two O···Li bonds have very similar lengths of 1.93 Å. Additionally,

TABLE 1: Calculated Results for Lithium Alkyl Dicarbonates at the B3PW91/6-31G(d) Level Including Total Binding Energies (TBE, kcal/mol), BSSE (kcal/mol), BSSE-Corrected Binding Energies [TBE(BSSE), kcal/mol), ZPE-Corrected Binding Energies [TBE(ZPE), kcal/mol), Variations of the Total Overlap-Weighted NAO Bond Orders for the Involved Li Ions ($\Delta\alpha$) and Variations of the Total Partial Charges from NPA for Li Ions ($-\Delta Q/E$)

structures	TBE[a]	BSSE	TBE(BSSE)[b]	TBE(ZPE)[c]	BE[d]	$\Delta\alpha$[e]	$-\Delta q$
1b	48.4	5.1	43.3	47.9	42.8	0.206	0.036
1c	46.4	8.8	37.6	45.8	37.0	0.170	0.042
1d	79.4	10.5	68.9	77.6	67.1	0.414	0.076
1e	97.2	13.4	83.8	95.6	82.2	0.356	0.064
1f	100.9	17.7	83.2			0.379	0.084
1g	133.1	23.1	110.0	132.8	109.7	0.450	0.063
1h	135.3	23.3	112.0			0.594	0.130
1i	153.5	25.4	128.1			0.631	0.115
1j	179.00	19.9	159.1	175.7	155.8	0.753	0.180
1k	145.4	16.9	128.5			0.562	0.100
1l	182.6	30.0	152.6	178.8	148.8	0.600	0.091
1m	236.2	33.6	202.6	232.1	198.5	1.032	0.231
2b	48.2	5.0	43.2	47.7	42.7	0.207	0.036
2c	46.3	8.8	37.5			0.172	0.041
2d	107.2	12.2	95.0	104.7	92.5	0.487	0.102
2e	96.3	10.1	86.2			0.410	0.074
2f	170.5	25.3	145.2	166.6	141.3	0.773	0.180
3b	49.1	5.2	43.9	48.4	43.2	0.211	0.038
3c	95.5	10.8	84.7	93.5	82.7	0.412	0.076
3d	98.1	10.4	87.7	96.8	86.4	0.417	0.074
3e	147.3	20.8	126.5			0.533	0.091
3f	187.5	21.2	166.3	183.4	162.2	0.727	0.167
3g	147.0	15.7	131.3			0.624	0.114
3h	253.0	35.6	217.4			0.996	0.217
3i	49.4	5.2	44.2	48.6	43.4	0.216	
4b	49.1	5.2	43.9	48.4	43.2	0.212	0.038
4c	103.8	13.1	90.7	101.5	88.4	0.481	0.101
4d	98.0	10.3	87.7			0.418	0.082
4e	182.3	25.2	157.1	178.8	153.6	0.738	0.170
4f	246.8	37.1	209.7				

[a] TBE = n*E(monomer) − E(n-mer). [b] TBE(BSSE) = TBE − BSSE. [c] TBE(ZPE), TBE with ZPE corrections. [d] BE, TBE with BSSE and ZPE. [e] $\Delta\alpha = \Sigma_j\alpha_j - m\alpha$ (m, the number of Li ions).

a six-membered ring occurs in the center of trimer **1j**, which is reflected by the considerable NBO bond orders of 0.08 for the three longer O···Li bonds (2.06−2.07 Å) and 0.11 for the other three shorter O···Li bonds (∼1.93 Å). It looks like that the three inner Li ions are shared by the four adjacent oxygen atoms. Besides considerable NBO bond orders, the four ionic O···Li bonds (two strong and two weak) are also supported by the AIM results, for example, the low electron density ρ (0.016, 0.021, 0.027, 0.028 au) and positive $\nabla^2\rho$ (0.11, 0.14, 0.20, 0.21 au) at the bond critical points. The outer Li ions are only shared by three oxygen atoms (two strong and one weak O···Li). As a result of this, the overall bond orders of the inner Li cations are higher those of the outer ones (0.405 vs 0.358). **1j** is the most stable structure among the trimer isomers (BSSE-corrected BE, 159.1 kcal/mol, see Table 1), followed by the closed structure **1i** (BE, 128.1 kcal/mol). The binding energies of **1h** and **1g** are very similar (112.0 and 110.0 kcal/mol), and the two open isomers, **1e** and **1f**, are the least stable (BE: 83.8 and 83.0 kcal/mol).

Regarding the tetramers, we focused on the open planar **1k**, the cagelike **1l**, and the closed pseudoplanar **1m**. As illustrated in Figure **1k**, the middle eight-membered ring consists of two nearly equal O···Li···O interactions ($\angle$O···Li···O = 161.1°, $r_{O\cdots Li}$ = 1.802 and 1.882 Å; $\angle$O···Li···O = 162.6°, $r_{O\cdots Li}$ = 1.804 and 1.889 Å), whereas the two end eight-membered rings resemble those in trimer **1b**; that is one O···Li···O approaches

TABLE 2: Thermodynamics for the Growth Reactions of Lithium Alkyl Dicarbonates [Total Energy Difference (ΔE, kcal/mol), ZPE-Corrected ΔE (ΔE_0), Change of Enthalpy at 298.15 K (ΔH), and Change of Gibbs Free Energies at 298.15 K (ΔG)]

growth reactions	ΔE	ΔE_0	ΔH	ΔG
1a + **1a** → **1d**	−79.4	−77.6	−77.8	−62.7
1a + **1d** → **1j**	−99.6	−98.2	−98.4	−83.1
1a + **1j** → **1m**	−57.2	−56.4	−55.8	−44.0
2a + **2a** → **2d**	−107.2	−104.7	−105.5	−87.5
2a + **2d** → **2f**	−63.3	−61.9	−61.8	−50.6
3a + **3a** → **3c**	−95.5	−93.5	−93.9	−78.3
3a + **3c** → **3f**	−91.9	−89.9	−90.5	−73.7
3a + **3f** → **3h**	−65.5			
4a + **4a** → **4c**	−103.8	−101.5	−102.3	−84.3
4a + **4c** → **4e**	−78.5	−77.2	−77.0	−63.5
4a + **4e** → **4f**	−64.6			

linear conformation ($\angle$O···Li···O = 176°, $r_{O\cdots Li}$ = 1.815 and 1.927 Å) and the other one dramatically bends to approximately 135° ($r_{O\cdots Li}$ = 1.778 and 1.822 Å). Like the cage trimer **1g**, the cage tetramer **1l** also possesses high symmetry (C_{4v}) and has two kinds of O···Li···O interaction ($\angle$O···Li···O = 138.0° and 154.7°) with equal O···Li bonds (1.791 and 1.815 Å, respectively) in each eight-membered ring. In the case of the pseudoplanar tetramer **1m**, the inner O···Li···O interactions are more bent than the outer ones to adopt higher coordination with adjacent oxygen atoms. Again, the closed pseudoplanar is the most stable isomer, the chain the least stable, and the cage isomer between. This indicates that LVD would grow from dimer **1d** to the closed pseudoplanar trimer **1j** and then to the closed tetramer **1m**, with a closed structure growth pattern. Thermodynamics for the growth reactions of lithium alkyl dicarbonates are summarized in Table 2. The high negative ΔG values also show that LVDs tend to associate, forming high-order structures.

Lithium Divinylene Dicarbonate (LDVD). Except for the presence of the longer conjugated $-(CH{=}CH-)_2$ group, its side-by-side dimer (**2c**, not shown) as well as chain dimer **2b** (Figure 2 the b) structures and binding energies are rather close to their analogues of lithium vinylene dicarbonate. However, dimer **2d** looks pronouncedly different from the cage dimer **1d**. The two inner Li ions are more strongly linked with the three adjacent oxygen atoms than the two outer Li ions. Consequently, the overall bond orders of the inner Li cations are higher than the outer Li cations (0.40 vs 0.35). In contrast to the chain trimer of lithium vinylene dicarbonate **1e**, no significant differences are found for O···Li···O interactions in the chain trimer (**2e**), although they are also somewhat different ($\angle$O···Li···O = 159.1° and 163.6°). Despite larger deviations from the planar structure compared to trimer **1j**, the corresponding pseudoplanar trimer has also been found, as shown in Figure **2f**. Similarly, a six-membered ring also exists in the trimer center, which contributes to the extra stability of the isomer **2f**.

Lithium Ethylene Dicarbonate (LED). The chain and cagelike dimers, **3b** and **3c**, have also been located for LED, whereas the stationary point corresponding to the side-by-side type of dimer was not found. The two degenerate O···Li···O interactions in **3b** are very similar to those in **1b** as well as in **2b** with an angle of 163.2°, a contracted Li···O bond (1.804 Å) and a stretched one (1.890 Å). The BSSE-corrected binding energy is only slightly higher than that in **1b** and **2b** (43.9, vs 43.2 and 43.3 kcal/mol). Like the cage dimer of lithium vinylene dicarbonate, **1d**, the four O···Li···O interactions in the cage dimer **3c** are also similar ($\angle$O···Li···O = 152.5−153.1°, $r_{O\cdots Li}$ = 1.906 and 1.822 Å); however, the angle of O···Li···O is slightly larger, by approximately 4°, than that in dimer **1d**. The

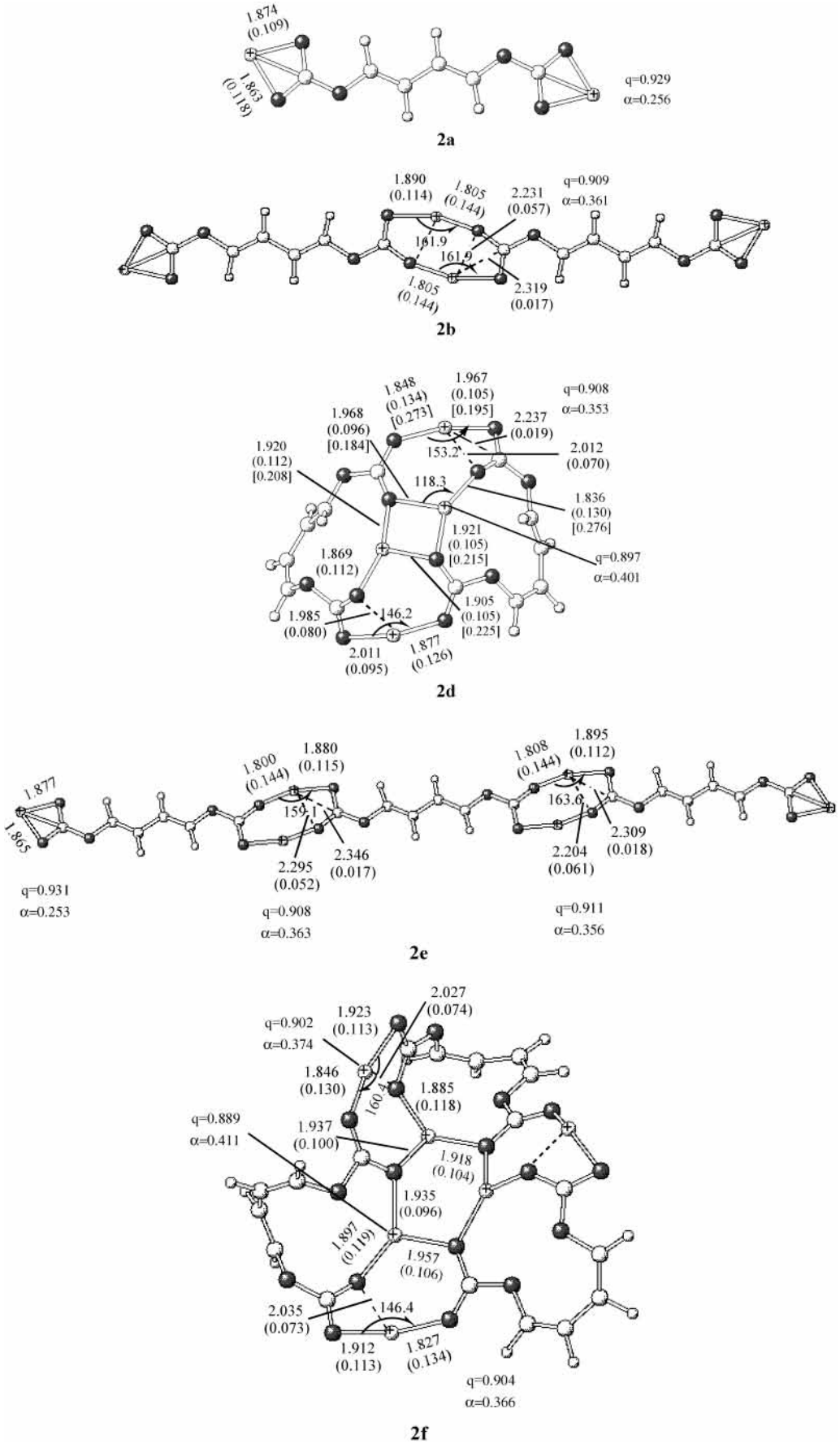

Figure 2. Structures with selected parameters by B3PW91/6-31G*: (**2a**) lithium divinylene dicarbonate; (**2b**, **2d**) dimer; (**2e**, **2f**) trimer. The symbols and notations have the same meaning as those in Figure 1.

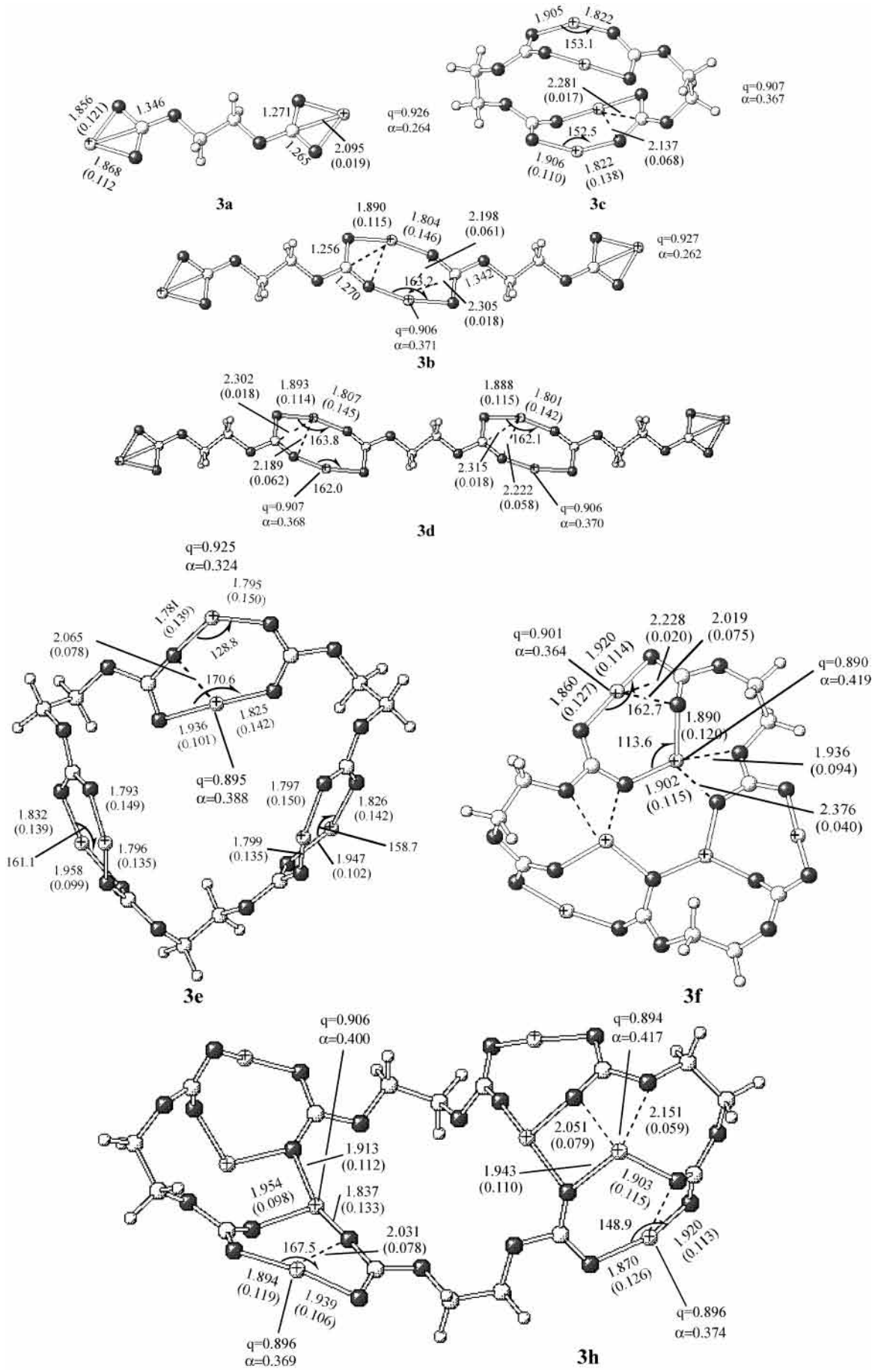

Figure 3. Structures with selected parameters by B3PW91/6-31G*: (**3a**) lithium ethylene dicarbonate; (**3b**, **3c**) dimer; (**3d**−**3f**) trimer; (**3h**) tetramer. The symbols and notations have the same meaning as those in Figure 1.

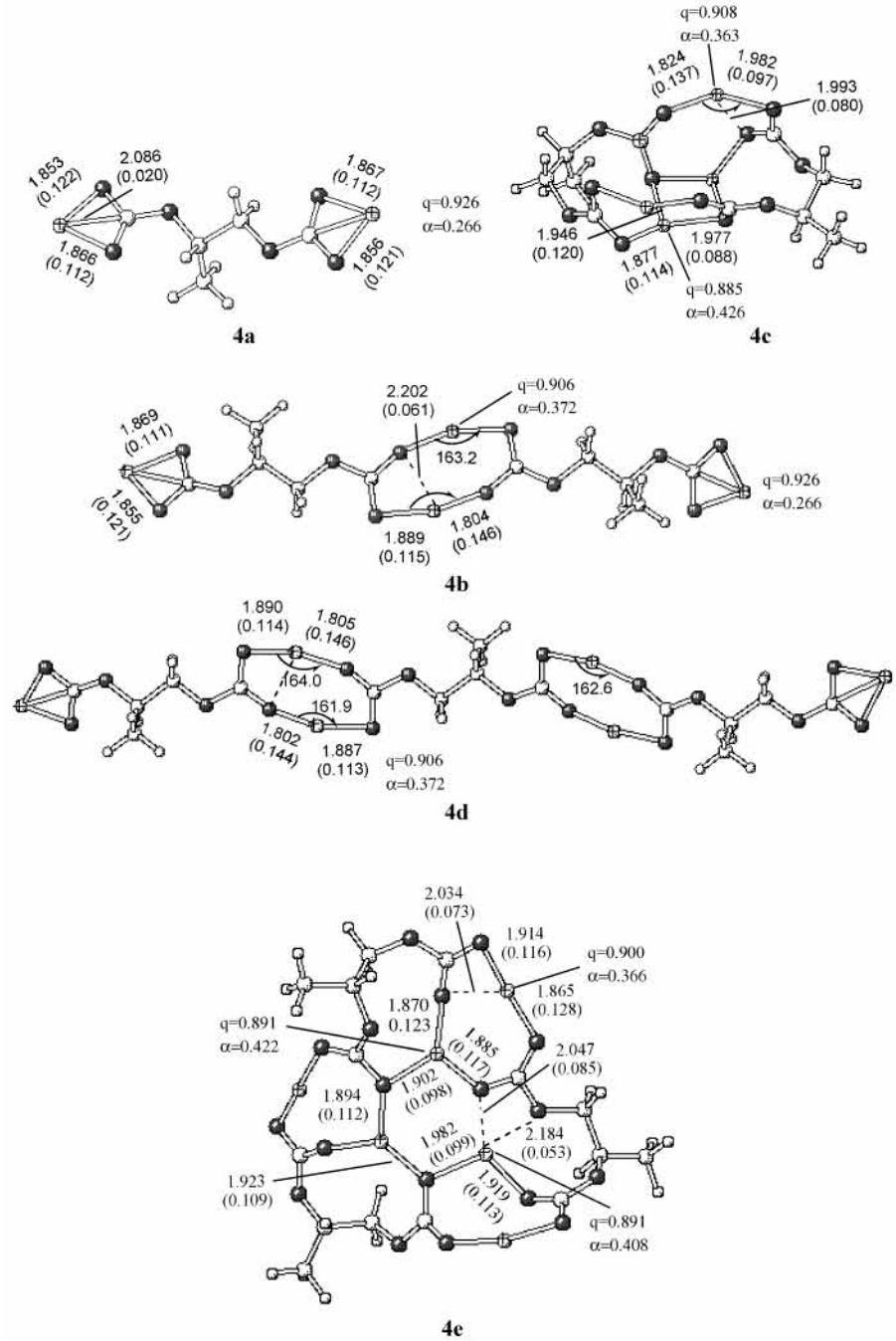

Figure 4. Structures with selected parameters by B3PW91/6-31G*: (**4a**) lithium propylene dicarbonate; (**4b**, **4c**) dimer; (**4d**, **4e**) trimer. The symbols and notations have the same meaning as those in Figure 1.

O···Li···O interactions in the chain trimer **3d** resemble those in dimer **3b**. The binding energy of the cagelike trimer **3e** is 38.8 kcal/mol higher than that of **3d** due to the presence of more O···Li···O interactions. The corresponding closed pseudoplanar trimer **3f** remarkably twists but still has the highest binding energy among the trimers. The O···Li···O interactions in the chain tetramer **3g** (not shown in Figure 3) are rather similar to those of its chain trimer **3d** and have a much lower binding energy than the closed pseudoplanar trimer **3h** (131.3 vs 217.4 kcal/mol).

Lithium Propylene Dicarbonate (LPD). The effect that the methyl group in lithium propylene dicarbonate has on its chain dimer **4b** (Figure 4b) as well as on the chain trimer **4d** (Figure 4d) is almost negligible. The O···Li···O interactions in **4b** are almost identical to those of **3b**, and those of **4d** and **3d** are also very similar. Their similarities are also reflected by the identical binding energies, 43.9 kcal/mol, for the chain dimers **3b** and **4b**, 87.7 kcal/mol for the chain trimers **3d** and **4d**. However, the cagelike dimer **4c** is much different from **3c**. The O···Li···O interactions of **4c** are more bent, and two of Li cations are shared by three neighbor oxygen atoms. As a result of the higher coordination in **4c**, the binding energy is 6.0 kcal/mol higher than that of **3c** (90.7 vs 84.7 kcal/mol). The closed trimer **4e** as well as the closed tetramer **4f** (not shown) corresponding to the previous pseudoplanar structures of LVD and LED were also located.

In summary, several lithium alkyl dicarbonates are able to associate through O···Li···O interactions, which could be classified as ionic bonding. The binding energies are somewhat different, for example, they are 159.1, 145.2, 166.3 and 157.1 kcal/mol for the closed pseudoplanar trimers, **1j**, **2f**, **3f**, and **4e**, of lithium alkyl (vinylene, divinylene, ethylene, and propylene)

TABLE 3: Characteristics for LVL Dimer, Water Dimer, and NaCl Dimer, Including HOMO (au), the Overall Bond Order (α), and Partial Atomic Charge (*q*) for the Interaction Donor Atoms Such as Li, H, and Na, Electrostatic (ES/au) Interaction between Donor Atoms and Neighbor Atoms.

	HOMO	α	Δα	*q*	Δ*q*	ES
LVL	−0.20583	0.256		+0.929		−0.20936
1b	−0.21561	0.362	0.106	+0.909	−0.020	−0.20618
1d	−0.24230	0.360	0.104	+0.910	−0.019	
H_2O	−0.29257	0.556		+0.471		
H_2O dimer	−0.26527	0.616	0.060	+0.489	+0.018	
NaCl	−0.22342	0.258		+0.901		−0.1805
NaCl dimer	−0.18758	0.325	0.067	+0.893	−0.008	−0.2573

dicarbonate. The energy difference between isomers for a given *n*-mer of a specific dicarbonate shows that lithium dicarbonate would grow, adopting the closed structure conformation, that is they would associate to the cagelike dimer first, then to the closed pseudoplanar trimer, then to the closed tetramer, and so on.

3.2. Partial Atomic Charges, Overall Bond Orders of Li Cations, and Binding Energies. Figures 1−4 show that upon formation of the intermolecular O···Li···O interactions, the partial atomic charges (*q*) of the Li cations decrease a little, and they are accompanied by increases of their overall bond orders (α). *q* in Li is decreased by 0.02e in **1d** (0.910e vs 0.929e); for example, an overall bond order α is increased by 0.104 (0.360 vs 0.256). In the case of lithium vinylene dicarbonate trimer **1j**, *q* and α for the outer Li cations are 0.904e and 0.358, respectively, whereas they are 0.894e and 0.405 for the inner Li cations. Except for the rather bent O···Li···O interactions having a higher charge *q* (0.93e) and lower α (0.32−0.33), such as those of the chain trimer (**1e**), cage trimer (**1g**), and tetramer (**1k**) of lithium vinylene dicarbonate, the partial atomic charges of Li generally lie in the range 0.91−0.89e, and the overall bond orders range from 0.36 to 0.41.

The decreases of the partial atomic charge in Li imply that Li···O loses polarity to some extent, whereas the increases of overall bond order imply that the covalent characteristics are increased even though Li···O are still ionic bonds as characterized by the positive $\nabla^2\rho$ at the bond critical points of Li···O. It is worth notice that the variation pattern of the partial charge of the Li ion is opposite to the conventional H-bond in which the partial charge of the donor H atom is increased upon the formation of the H-bond, for example, it is increased from 0.471e to 0.489e for the H_2O dimer with NPA/B3PW91/6-31G*//B3PW91/6-311++G(d,p). However, the overall NBO bond order for the H-bond donor H atom is also definitely increased (0.616 vs 0.556).

To get insights into the origin of the binding energies of the lithium dicarbonate complexes, a parallel investigation has been done for dimerization of a typical ionic compound, NaCl. From Table 3, the bond order α and the partial atomic charge for the interaction donor Na qualitatively have the same variation pattern; however the variations are about 1 time less than those of lithium vinylene dicarbonates. Both the HOMO and electrostatic (ES) attractions between the donor Li/Na and its neighbor atoms behave oppositely for LVL and NaCl dimers. As expected, the ES attraction in the NaCl dimer becomes more negative, which together with the increase of the HOMO shows that electrostatic forces dominate in the NaCl complex. On the contrary, approximately 2 kcal/mol decrease of the ES attraction for each donor Li ion is found in dimer **1b**, and the considerable decrease of the HOMO implies that ES forces may be not important as that in the NaCl dimer, and that covalent characteristics perhaps play a very important role in stabilizing

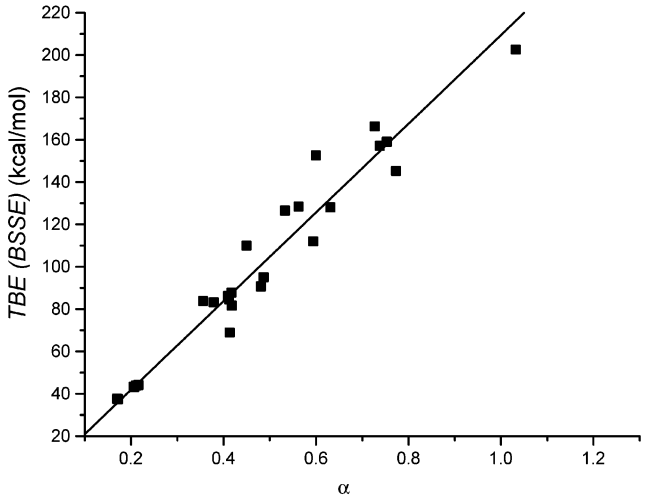

Figure 5. BSSE-corrected binding energies [TBE(BSSE), kcal/mol] against the total variations of overall bond orders (Δα) for the involved Li ions. Square symbols refer to those from NBO-B3PW91/6-31G; the solid line is the linear fitted results (correlation coefficient ∼ 0.98).

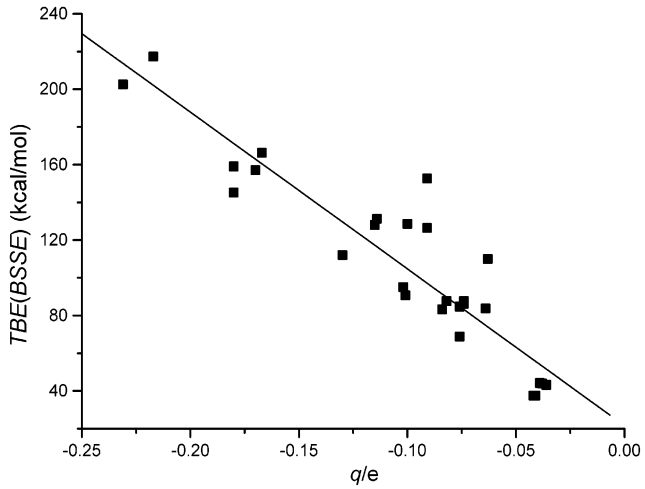

Figure 6. BSSE-corrected binding energies [TBE(BSSE), kcal/mol] against the total variations of partial charges (*q*) for the involved Li ions. Square symbols refer to those from NPA-B3PW91/6-31G; the solid line is the linear fit with a correlation coefficient of 0.93.

lithium dicarbonate complexes. Further, close inspections show that the binding energies with BSSE correlation linearly correlate (correlation coefficient ∼ 0.98) with the total increase of the overall bond orders (Δα) of Li ions, as illustrated in Figure 5. It is noted that the linear correlation between binding energies with total variation of *q* (Figure 6, correlation coefficient ∼ 0.93) indeed is not as good as with that of overall bond orders, although the decrease of the partial charges of Li ions also closely associates with the formation of O···Li···O systems.

3.3. Vibrational Frequencies. FTIR is one of the most common tools used to identify the SEI components, the vibrational frequencies with IR activity for the relevant monomers and aggregates are therefore presented to make a sensible comparison with experiments and eventually to comprehensively identify the SEI composition. First of all to get a reasonable scaling factor for the used method, frequency analyses were done at the B3PW91/6-31G(d) level for the monomers as well as dimers of lithium methyl, ethyl, and propyl carbonate ($MeOCO_2Li$, $EtOCO_2Li$, $PrOCO_2Li$), experimental data of which are available. Despite about a 7 cm^{-1} increase arising from dimerization of $MeOCO_2Li$ (maximal absorption 3187 vs

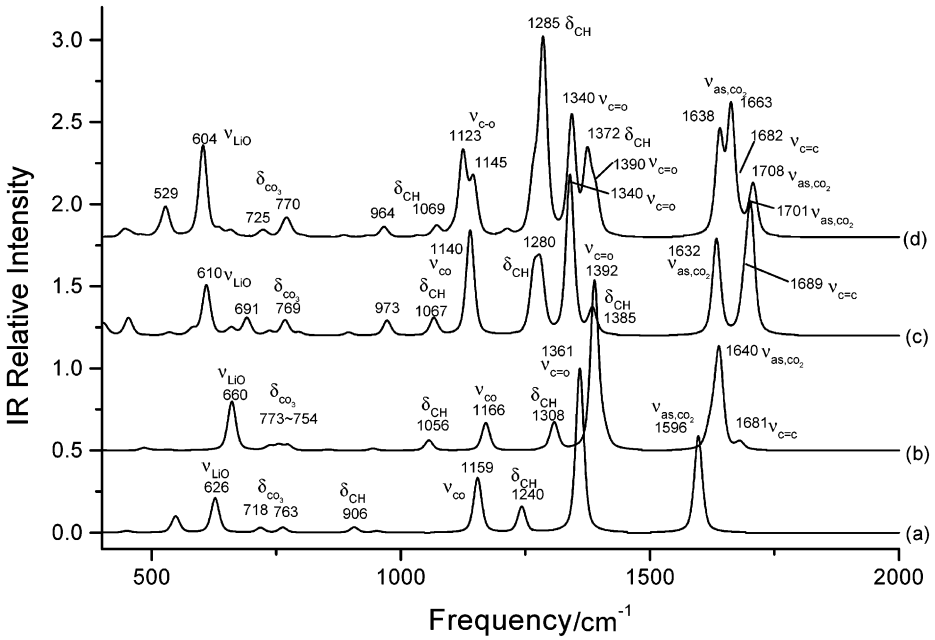

Figure 7. Simulated infrared spectra for lithium vinylene dicarbonate **1a** (a), dimer **1d** (b), trimer **1j** (c), and tetramer **1m** (d) with parameters: 50% Gaussian + 50% Lorentzian functions, 20 cm^{-1} peak width; frequencies and relative intensities based on QC calculations of B3PW91/6-31G(d) with a scaling factor of 0.949.

3180 cm^{-1}), CH_3 and/or CH_2 stretching frequencies increase by no more than 2 cm^{-1} for the dimerizations of $EtOCO_2Li$ and $PrOCO_2Li$ (3159 vs 3157 and 3141 vs 3139 cm^{-1}). The corresponding maximal CH_3/CH_2 stretchings on a lithium metal surface are 3021, 2976, and 2980 cm^{-1};[9] thus the averaged scale factor for the three carbonates is 0.949, which is close to the empirical factor 0.96 suggested by Curtiss et al. for B3LYP/6-31G(d) method.[28]

Figure 7 presents the simulated infrared spectra of lithium vinylene dicarbonate, and its dimer (**1d**), trimer (**1j**), and tetramer (**1m**). The most significant changes associated with aggregation are (i) the asymmetric CO_2 stretching ($\nu_{as,CO2}$) shifts from 1596 cm^{-1} of monomer to 1640 cm^{-1} of dimer **1d**. In the cases of trimer **1j** and tetramer **1m**, there are two (1701 and 1632 cm^{-1}) and three (1708, 1663 and 1638 cm^{-1}) peaks assigned to $\nu_{as,CO2}$, respectively, which certainly overlap each other, forming one peak if the line width is taken over 33 cm^{-1} in the simulation. (ii) A new weak peak assigned to C═C stretching (νc═c) occurs at 1681 cm^{-1} in Figure 7b of dimer **1d** due to the appearance of double bond polarity but is covered by stronger $\nu_{as,CO2}$ in the cases of trimer (1689 cm^{-1}, medium) and tetramer (1682 cm^{-1}, medium). (iii) The C═O stretching peak (νc═o), which was usually identified as symmetry stretching of CO_2 by experimentalists,[5] and the C−H in-plane bending peak (δ_{CH}) also yield blue shifts from monomer to dimer **1d** (ν_{CO}, 1361 vs 1392 cm^{-1}; δ_{CH}, 1240 vs 1308 cm^{-1}). However, they are no longer well separated in Figure 7c of trimer **1j** and in Figure 7d of tetramer **1m**, and even considerably coupled to each other in **1m**. (iv) The Li−O stretching (ν_{OLi}) goes through a blue shift from monomer to dimer **1d** (ν_{OLi}, 626 vs 660 cm^{-1}) and then red shifts to the trimer and tetramer (610 and 604 cm^{-1}), which is in line with the variations of Li−O bond lengths. Other vibrational modes such as C−H stretching ($\nu_{CH} \sim 3100$ cm^{-1}) that will be shown in Figure 11, C(alkyl carbon)−O stretching ($\nu_{CO} \sim 1160$ cm^{-1}), C−H out-of-plane bending ($\delta_{CH} \sim 906$ cm^{-1}, weak) and CO_3 bending ($\delta_{CO3} \sim 770$ cm^{-1}), show only a small change due to association.

Figure 8 shows the simulated infrared spectra of lithium divinylene dicarbonate, its dimer (**2d**), and the trimer (**2f**). Considerable blue shifts also take place on $\nu_{as,CO2}$, 1597, 1662, and 1685−1667 cm^{-1} for the monomer, dimer, and trimer, respectively. A weak C═C stretching peak appears at 1628 cm^{-1} in Figure 8a of the monomer. It splits and shifts to higher frequencies, 1622 and 1640 cm^{-1} for the dimer, 1651 and 1665 cm^{-1} for the trimer, which are covered by stronger $\nu_{as,CO2}$. Compared with those of lithium vinylene dicarbonate trimer **1j**, the νc═c mode of trimer **2f** has an over 20 cm^{-1} red shift (1651−1665 vs 1689 cm^{-1}). Like the case of lithium vinylene dicarbonate, C═O stretching (νc═o) and C−H in-plane bending peak (δ_{CH}) strongly couple in the dimer (Figure 8b) as well as in the trimer (Figure 8c). The rest of the variations, such as Li−O stretching (ν_{OLi}), C−O (alkyl carbon) stretching (ν_{CO}), and CO_3 bending ($\delta_{CO3} \sim 770$ cm^{-1}), are also very similar to the patterns of those displayed in Figure 7.

The effects of association on the infrared spectra of lithium ethylene dicarbonate and lithium propylene dicarbonate are displayed in Figures 9 and 10, respectively. Associations lead to changes similar to those observed for lithium vinylene dicarbonate and lithium divinylene dicarbonate. In the range of 1600−1700 cm^{-1}, vibrational peaks only relate to CO_2 asymmetric stretching because of the absence of C═C bonds. Additionally, CH_2 and/or CH_3 bending, such as scissoring, rotating, and wagging, couple so strongly with C═O stretching around 1400 cm^{-1} that there are no separate peaks assigned to ν_{CO} and δ_{CH} even for their monomers. Aurbach et al. [9] measured IR bands of lithium propylene dicarbonate and made the assignments as follows: ν_{C-H} 2990 m, 2950 m, 2870 w; $\nu_{as,CO2}$ 1665 s, 1540 s; $\delta_{CH,CH3}$ 1430 s; $\nu_{s,CO2}$ 1330 m; ν_{C-O} 1200 w, 1150 m, 1100 sh, 1070 sh, 1050 s; δ_{CH2} 920 w; δ_{CO3} 870 s, 830 m; δ_{CO2} 750 w, 650 w; ν_{Li-O} 520 s. Besides the ν_{C-H} (2997, 2946, and 2924 cm^{-1}) that will be shown in Figure 11, the simulated results in Figure 10c basically agree with Aurbach's experimental results, especially with respect to the leading peak groups, that is ν_{C-H}, $\nu_{as,CO2}$ (1682−1619 cm^{-1}), $\delta_{CH,CH3}$ (∼1430), $\nu_{c=o}$ (∼1330), ν_{C-O} (1082−1110), δ_{CO3} (784), δ_{CO2} (670−694), and ν_{Li-O} (614−642), even though minor differences still exist on details of the spectra.

Comparisons are made in Figure 11 between the IR spectra

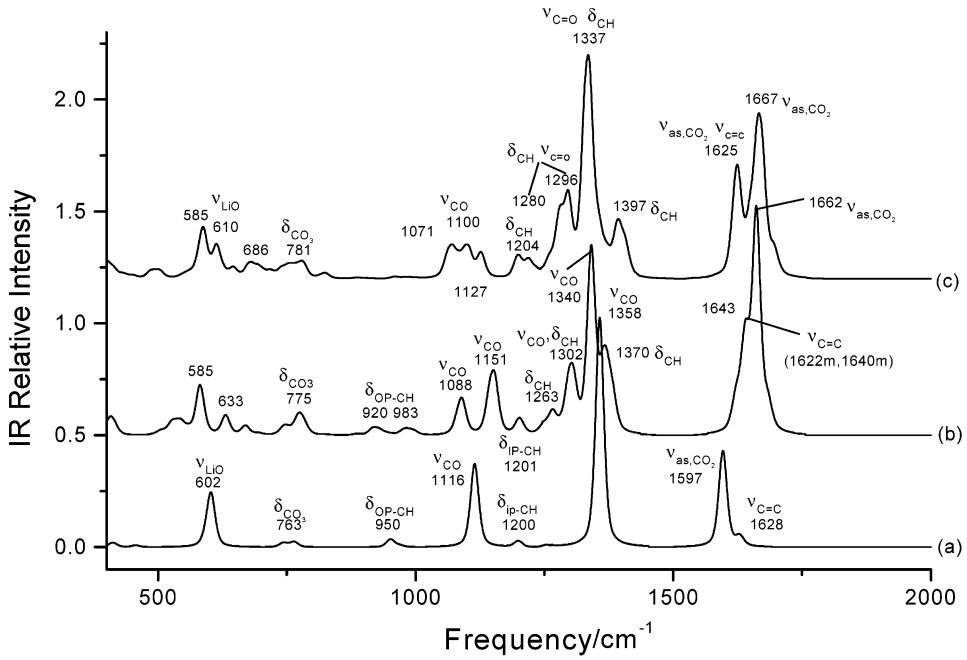

Figure 8. Simulated infrared spectra for lithium divinylene dicarbonate **2a** (a), dimer **2d** (b), and trimer **2f** (c) with the same parameters as in Figure 7.

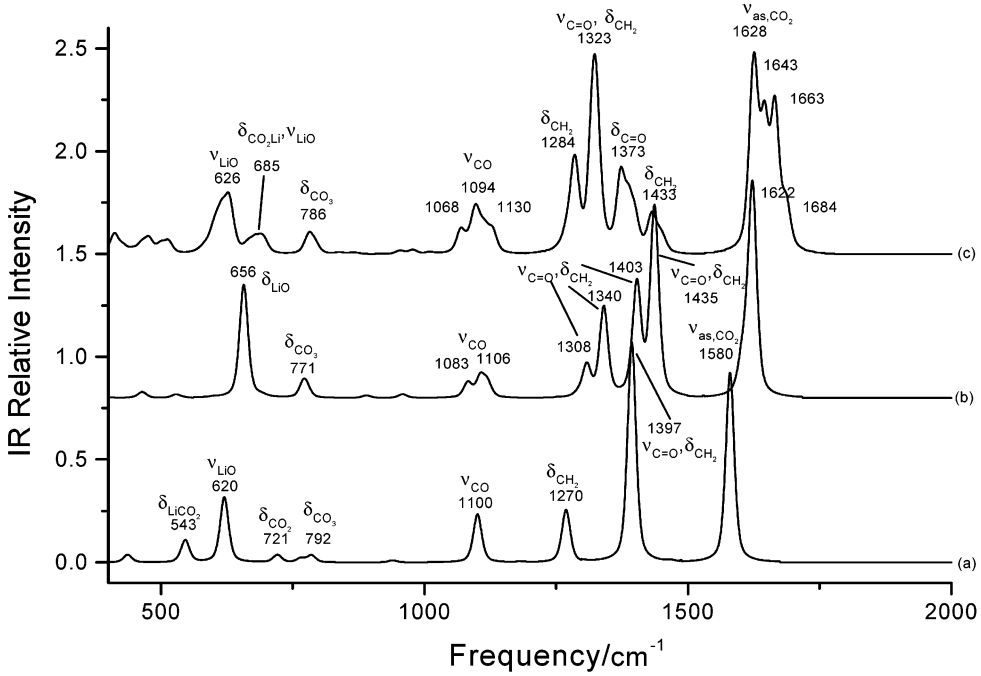

Figure 9. Simulated infrared spectra for lithium ethylene dicarbonate **3a** (a), dimer **3c** (b), and trimer **3f** (c) with the same parameters as in Figure 7.

of the four lithium alkyl (vinylene, divinylene, ethylene, and propylene) dicarbonates in the range 400−3200 cm^{-1}. C−H stretching vibrations of the two unsaturated lithium dicarbonates are weaker than those of lithium ethylene/propylene dicarbonate, and the frequencies of the former are higher by about 90 cm^{-1} than those of the latter (3074−3104, 3031−3092 vs 2943−3011, 2924−2997 cm^{-1}), which is one of the pronounced features that could be used to determine whether double bond-containing species are present on the SEI layer. Bending of $CH/CH_2/CH_3$ (δ_{CHn}) is another clear difference, 1385 cm^{-1} for **1j**, 1397 cm^{-1} for **2f**, 1433 cm^{-1} for **3f**, and 1442 cm^{-1} for **4e**, but is usually covered by the stronger C−O stretching (ν_{CO}) with approximate 40−60 cm^{-1} lower frequency. As discussed above, peaks related to C═C stretching are definitely determined with DFT calculations around 1680 cm^{-1} for vinylene dicarbonate and 1620−1650 cm^{-1} for divinylene dicarbonate, respectively; however they are not well separated from stronger $\nu_{as,CO2}$. Because it is commonly known that high-order conjugation moves νc═c to the lower frequency and increases its intensity, which is also reflected by the present difference between vinylene dicarbonate and divinylene dicarbonate, it is expected that the unsaturated lithium dicarbonates, $LiOCO_2(CH{=}CH)_nOCO_2Li$ with higher order $n > 2$ would lead to separation of the C═C stretching peaks with frequencies lower than 1620 cm^{-1}. This argument roughly supports Aurbach's conclusion,[13] on the basis of the fact that the IR peaks are found between 1570 and 1610 cm^{-1},

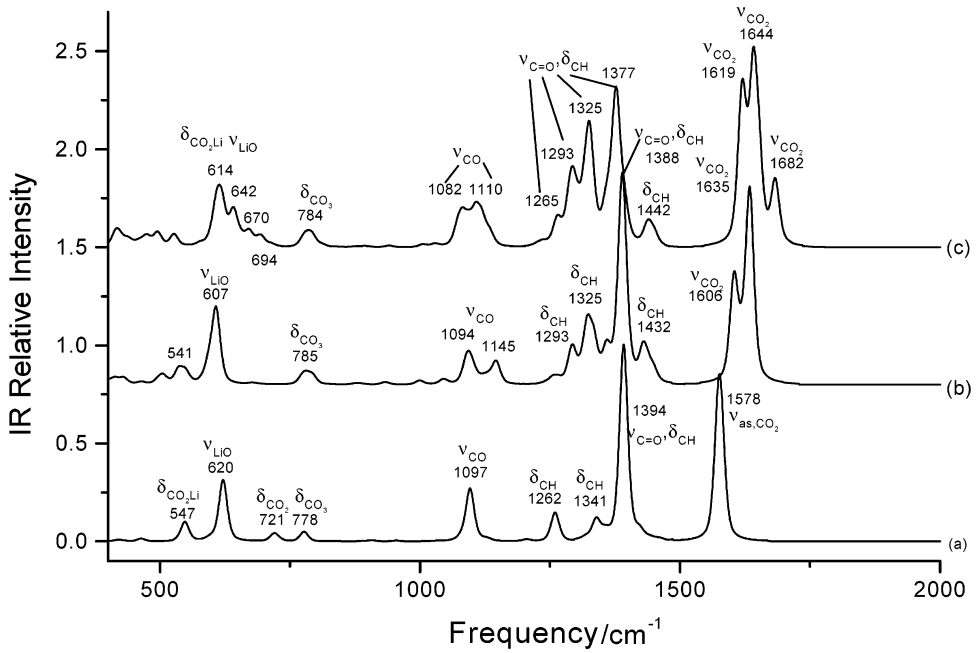

Figure 10. Simulated infrared spectra for lithium propylene dicarbonate **4a** (a), dimer **4c** (b), and trimer **4e** (c) with the same parameters as in Figure 7.

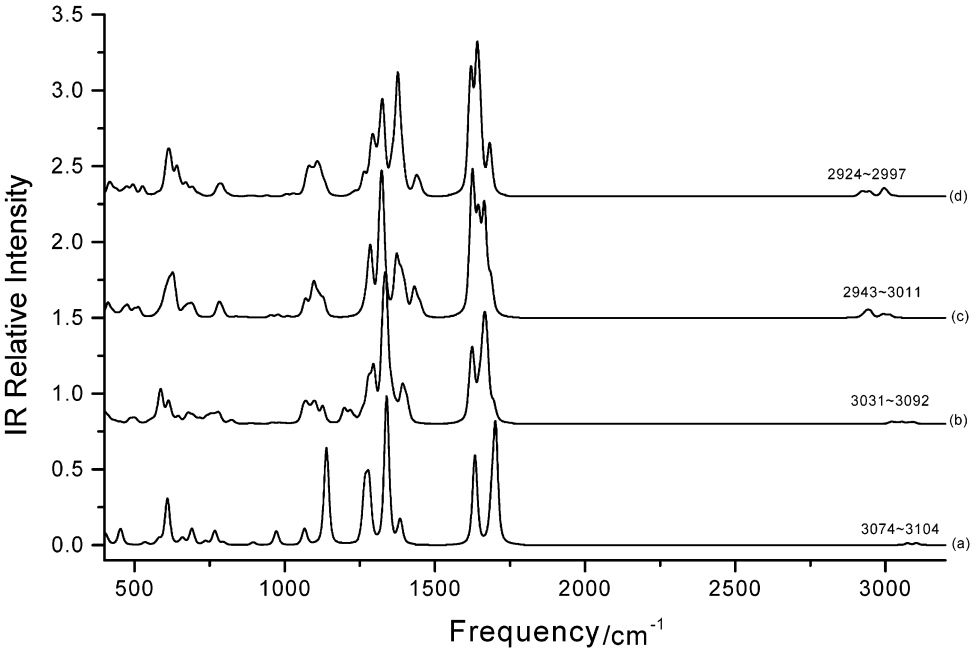

Figure 11. Comparisons of the simulated spectra between the lithium vinylene dicarbonate trimer **1j** (a), lithium divinylene dicarbonate trimer **2f** (b), lithium ethylene dicarbonate trimer **3f** (c) and lithium propylene dicarbonate **4e** (d).

that the SEI layer contains polymeric species of polyvinylene dicarbonate in VC-containing electrolyte solutions.

4. Conclusions

Density functional theory-based methods have been utilized to investigate associations of lithium alkyl (vinylene, divinylene, ethylene, and propylene) dicarbonates, including geometry optimizations, frequency calculations, and bonding characterizations with the state-of-the-art AIM and NBO approaches. Lithium alkyl dicarbonates could associate through intermolecular O···Li···O interactions.[29] The global minima were found to be the cagelike isomer for dimers and closed pseudoplanar structures for trimers and tetramers, respectively. We can conclude that once these products are formed near the surface of the anode, they will deposit on the surface in the form of these 2-dimensional associates and even 3-dimensional ones, which generate monolayer and multilayer SEI, respectively. On the basis of AIM and NBO results, O···Li···O_x (x = 1−3) interactions could still be classified as ionic bonds even though polarities of Li···O are considerably decreased, which is reflected by the fact that the partial charges of Li ions are lowered by about 0.004e to 0.035e upon forming O···Li···O interactions or by Li being shared by more adjacent oxygen atoms. Meanwhile, it has also been found that the overall NBO bond orders of Li are pronouncedly increased. Interestingly, the BSSE-corrected binding energies of the associates were found to linearly correlate with the total variations of bond orders of all the involved Li ions. Additionally, we found that the IR

spectrum caused by the associations of lithium alkyl dicarbonates becomes closer to the experimental data than that of the monomer. This fact further support the previous conclusion that lithium alkyl dicarbonate exists on the anode surface, forming associates such as dimers, trimers, tetramers, and even higher order *n*-mers rather than monomers.

Acknowledgment. This work was partially supported by NSF (Career Award Grant CTS-9876065 to P.B.B.) and by Mitsubishi Chemical Corp.

References and Notes

(1) Tarascon, J.-M.; Armand, M. *Nature* **2001**, *414*, 359.
(2) Schechter, A.; Aurbach, D.; Cohen, H. *Langmuir* **1999**, *15*, 3334.
(3) Bar-Tow, D.; Peled, E.; Burstein, L. *J. Electrochem. Soc.* **1999**, *146*, 824.
(4) Naji, A.; Ghanbaja, J.; Humbert, B.; Willmann, P.; Billaud, D. *J. Power Sources* **1996**, *63*, 33.
(5) Aurbach, D.; Levi, M. D.; Levi, E.; Schechter, A. *J. Phys. Chem. B* **1997**, *101*, 2195.
(6) Wang, Y. X.; Nakamura, S.; Ue, M.; Balbuena, P. B. *J. Am. Chem. Soc.* **2001**, *123*, 11708.
(7) Wang, Y. X.; P. B. Balbuena. *J. Phys. Chem. B* **2002**, *106*, 4486.
(8) Aurbach, D.; Weissman, I.; Schechter, A.; Cohen, H. *Langmuir* **1996**, *12*, 3991.
(9) Aurbach, D.; Daroux, M. L.; Faguy, P. W.; Yeager, E. *J. Electrochem. Soc.* **1987**, *134*, 1611.
(10) Jehoulet, C.; Biensan, P.; Bodet, J. M.; Broussely, M.; Tessier-Lescourret, C. *Batteries for Portable Applications and Electric Vehicles*; The Electrochemical Society Proceedings Series; Electrochemical Society: Pennington, NJ, 1997.
(11) Fujimoto, M.; Shouji, Y.; Nohma, T.; Nishio, K. *Denki Kagaku* **1997**, *65*, 949.
(12) Wang, Y. X.; Nakamura, S.; Tasaki, K.; Balbuena, P. B. *J. Am. Chem. Soc.* **2002**, *124*, 4408.
(13) Aurbach, D.; Gamolsky, K.; Markovsky, B.; Gofer, Y.; Schmidt, M.; Heider, U. *Electrochim Acta* **2002**, *47*, 1423.
(14) Jeong, S.-K.; Inaba, M.; Mogi, R.; Iriyama, Y.; Abe, T.; Ogumi, Z. *Langmuir* **2001**, *17*, 8281.
(15) Besenhard, J. O.; Fritz, H. P. *J. Electrochem. Soc.* **1974**, *3*, 329.
(16) Besenhard, J. O.; Winter, M.; Yang, J.; Biberacher, W. *J. Power Sources* **1995**, *54*, 228.
(17) Winter, M.; Besenhard, J. O. In *In Lithium Ion Batteries: Fundamentals and Performances*; Wakihara, M., Yamamoto, O., Eds.; Wiley-VCH: New York, 1999; p 127.
(18) Frisch, M. J.; Trucks, G. W.; Schlegel, H. B.; Scuseria, G. E.; Robb, M. A.; Cheeseman, J. R.; Zakrzewski, V. G.; Montgomery, J. A.; Stratmann, R. E.; Burant, J. C.; Dapprich, S.; Millam, J. M.; Daniels, A. D.; Kudin, K. N.; Strain, O. F. M. C.; Tomasi, J.; Barone, B.; Cossi, M.; Cammi, R.; Mennucci, B.; Pomelli, C.; Adamo, C.; Clifford, S.; Ochterski, J.; Petersson, G. A.; Ayala, P. Y.; Cui, Q.; Morokuma, K.; Malick, D. K.; Rabuck, A. D.; Raghavachari, K.; Foresman, J. B.; Ciolovski, J.; Ortiz, J. V.; Stefanov, V. V.; Liu, G.; Liashensko, A.; Piskorz, P.; Komaroni, I.; Gomperts, R.; Martin, R. L.; Fox, D. J.; Keith, T.; Al-Laham, M. A.; Peng, C. Y.; Nanayakkara, A.; Gonzalez, C.; Challacombe, M.; Gill, P. M. W.; Johnson, B.; Chen, W.; Wong, M. W.; Andres, J. L.; Head-Gordon, M.; Replogle, E. S.; Pople, J. A. *Gaussian98*, revision A.9; Gaussian Inc.: Pittsburgh, PA, 1998.
(19) Becke, A. D. *J. Chem. Phys.* **1993**, *98*, 5648.
(20) Perdew, J. P. Unified theory of exchange and correlation beyond the local density approximation. In *Electronic Structure of Solids*; Ziesche, P., Eschrig, H., Eds.; Akademie Verlag: Berlin, 1991.
(21) Burke, K.; Perdew, J. P.; Wang, Y. *Electronic Density Functional Theory: Recent Progress and New Directions*; Plenum: New York, 1998.
(22) Perdew, J. P.; Burke, K.; Wang, Y. *Phys. Rev. B* **1996**, *54*, 16533.
(23) Boys, S. F.; Bernardi, F. *Mol. Phys.* **1970**, *19*, 553.
(24) Reed, A. E.; Curtisss, L. A.; Weinhold, F. *Chem. Rev.* **1988**, *88*, 899.
(25) Breneman, C. M.; Wiberg, K. B. *J. Comput. Chem.* **1990**, *11*, 361.
(26) Bader, R. F. W. *Atoms in molecules, a quantum theory*; Clarendon Press: Oxford, U.K., 1990.
(27) Wang, Y. X.; Balbuena, P. P. *J. Phys. Chem. A* **2001**, *105*, 9972.
(28) Baboul, A. G.; Curtiss, L. A.; Redfern, P. C.; Raghavachari, K. *J. Chem. Phys.* **1999**, *110*, 7650.
(29) Upon request, coordinates of the optimized structure will be provided.